DOI: 10.1002/ejic.200900892

Enantiomerically Pure P,N Chelates Based on Phospholene Rings: Palladium Complexes and Catalytic Applications in Allylic Substitution

François Leca,[a] Fernando Fernández,[b] Guillermo Muller,[b] Christophe Lescop,[a] Régis Réau,*[a] and Montserrat Gómez*[b,c]

Keywords: Palladium / Asymmetric catalysis / Chiral resolution / P ligands / Allylic substitutions

The synthesis of optically pure 2-pyridylphospholene ligands by diastereomeric resolution of Pd^{II} complexes, bearing the corresponding racemic P,N ligand and (*R*)-α-methylbenzylamine, by means of fractional crystallisation is described. A full coordination study of palladium complexes containing 2-pyridylphospholene and the corresponding phosphole ligands, both in solution (by means of NMR spectroscopy) and in the solid state (by X-ray diffraction), was carried out. These ligands were evaluated in Pd-catalysed allylic substitution of racemic substrates (*rac*-3-acetoxy-1,3-diphenyl-1-propene and *rac*-3-acetoxy-1-cyclohexene) and (*E*)-3-acetoxy-1-phenyl-1-propene. A modelling study of the palladium allylic intermediates was performed in order to justify the asymmetric induction observed with the 2-pyridylphospholene ligands.

Introduction

The design of an asymmetric environment around a metallic centre in order to accommodate the partners of an organic transformation allows enantioselectivity induction in asymmetric catalytic processes.[1,2] A classical approach to get this goal is the use of enantiomerically pure ligands containing donor atoms with a defined symmetry, which combines steric hindrance and electronic effects.[3] The rigidity of the backbone is one of the key aspects to consider in the structure of chiral ligands. In particular, the coordinating heteroatom placed on a cyclic fragment (like pyridine, thiophene or phosphole derivatives) can play a crucial role in the asymmetric induction, from both an electronic and a steric point of view. With regard to P-donor ligands, the significant contribution of Burk and co-workers in the early nineties,[4] which describes phospholane ligands (saturated phosphorus-containingcations in several metal-catalysed processes.[5] Phospholes, the related unsaturated heterocycles, which exhibits different steric and electronic properties to those shown by phospholanes, have also been extensively applied in catalysis, often as hetero-donor ligands that contain an additional group, e.g. pyridine, oxazoline or phosphane derivatives, other than the phosphole-coordinating moiety.[6] However, 2-phospholenes (Figure 1), an intermediate between phospholanes and phospholes, have been rarely applied in catalysis probably because of their minor synthetic development relative to the other two related P heterocycles.[6b,7]

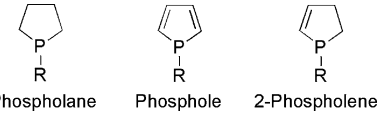

Figure 1. Skeletons of the phosphorus-containing five-membered heterocycles.

With respect to asymmetric catalytic applications of designed chiral ligands, enantioselective palladium-catalysed substitution of allylic substrates, a powerful synthetic tool for the enantioselective construction of carbon–carbon or carbon–heteroatom bonds, has proven to be a useful testing ground for the evaluation of new optically pure ligands.[8] For P-heterocycle-containing ligands, phospholes have led to moderate[9]-to-high (up to 90% *ee* for the alkylation of 1,3-diphenylprop-2-enylacetate[10]) enantiomeric excesses in Pd-catalysed allylic substitution reactions, in contrast to the excellent enantioselectivities induced by phospholane ligands.[11] To the best of our knowledge, there has only been one report on 2-phospholene ligands in asymmetric allylic substitution reactions; the results show a 95-% enantiomeric excess for the allylic amination of cyclopentenyl carbonate.[7c] Note that no P,N-chelate-bearing optically pure 2-phospholene moieties are known to date.

[a] UMR 6226 "Sciences Chimiques de Rennes, Université Rennes I, Campus de Beaulieu,
263 Av. du Général Leclerc, 35042 Rennes Cedex, France
Fax: +33-2-23236939
E-mail: regis.reau@univ-rennes1.fr
[b] Departament de Química Inorgànica, Universitat de Barcelona, Martí i Franquès, 1-11, 08028 Barcelona, Spain
[c] Laboratoire Hétérochimie Fondamentale et Appliquée, UMR CNRS 5069, Université Paul Sabatier,
118, route de Narbonne, 31120 Toulouse Cedex 9, France
Fax: +33-5-61558204
E-mail: gomez@chimie.ups-tlse.fr

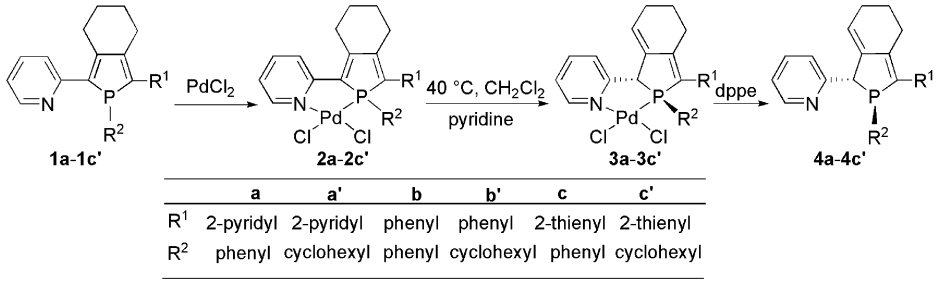

Scheme 1. Palladium-driven stereoselective synthesis of 2-pyridylphospholenes **4** from 2-pyridylphospholes **1**.

On the basis of these precedent research studies, we decided to isolate optically pure pyridylphospholene ligands, following the previous methodology described by some of us (Scheme 1),[7b] by means of the resolution of a diasteromeric mixture of Pd^{II} complexes. Application in Pd-catalysed allylic alkylation and amination has been carried out with the aim to evaluate the catalytic activity, enantioselectivity and regioselectivity. Modelling studies of palladium allyl intermediates have been performed in order to justify the asymmetric inductions obtained.

Results and Discussion

Synthesis of Ligands

We recently described a general and straightforward route to the first P,N chelates that incorporate phospholene moieties. This route involves the stereoselective isomerisation of Pd^{II}-coordinated 2-pyridylphosphole ligands into their corresponding 2-pyridyl-2-phospholene isomers in the presence of pyridine (Scheme 1).[7b] This synthetic approach is attractive given that (i) the isomerisation process is not sensitive to the nature of the P substituent and (ii) it is a highly stereoselective process that only affords isomers in which the pyridyl and the P substituent are in a mutual *trans* configuration (Scheme 1). The free 2-pyridylphospholenes could readily be obtained as a pair of enantiomers upon addition of 1 equiv. 1,2-(diphenylphosphanyl)ethane (dppe) to complexes **3a**–**3c′** (Scheme 1). Interestingly, no inversion of the stereogenic P centre occurs below 90 °C, which reveals that these derivatives are potentially attractive P-chiral, P,N chelates for homogeneous catalysis. The next step was thus to investigate the resolution of these readily available racemic 2-pyridyl-2-phospholene derivatives **4a**–**4c′**.

The first approach designed to obtain enantiomerically pure derivatives **4a**–**4c′** consisted of the protonation of the basic pyridyl moiety by chiral acids. *rac*-2-Pyridylphospholene (**4c**) was selected for this study. Its reaction with one equivalent of a chiral organic acid [(*S*)-mandelic acid, (*S*)-malic acid or (*S*,*S*)-dibenzoyl tartaric acid] afforded two diastereomeric pyridilium salts [$\delta(^{31}P)$ NMR: +26.7 and +26.5 ppm]. However, these 2-pyridiliumphospholenes are extremely air sensitive, which hinders the separation of the diastereomers upon fractional crystallisation. Therefore, an efficient strategy should prevent oxidation of the rather electron-rich P centre of derivatives **4**.

With this in mind, a second approach was investigated based on the resolution of Pd^{II} complexes **3** (Scheme 1), which are stable in air (the P atom is somehow protected from oxidation by coordination onto the metal centre). Our strategy involved the introduction of a novel enantiomerically pure ligand [(*R*)-α-methylbenzylamine] onto the metal centre in order to form diastereomers. Thus, complex **3a** [$\delta(^{31}P)$ NMR: +67.3 ppm] reacted with (*R*)-α-methylbenzylamine in the presence of silver hexafluorophosphate (Scheme 2), which gives the new complex **5a** as a mixture of two diastereomers, **5a¹** and **5a²** (89% yield). The $^{31}P\{^{1}H\}$ NMR spectrum of the crude reaction mixture displays two sharp singlet signals of equal intensity at +73.2 and +72.5 ppm (Figure 2a). Further, the ^{1}H and ^{13}C NMR spectra show two sets of signals corresponding to each diastereomer. Although the NMR spectroscopic data could not help to establish the relative position of the chlorine and amine ligands with respect to the P and N atoms, this could be determined by means of an X-ray diffraction study on diastereoisomer **5a¹** (vide infra). A similar behaviour was observed for complex **3a′**, which features a P-cyclohexyl phospholene ligand (Scheme 2). The resulting complex **5a′** was isolated as a 1:1 mixture of diastereoisomers [$\delta(^{31}P)$

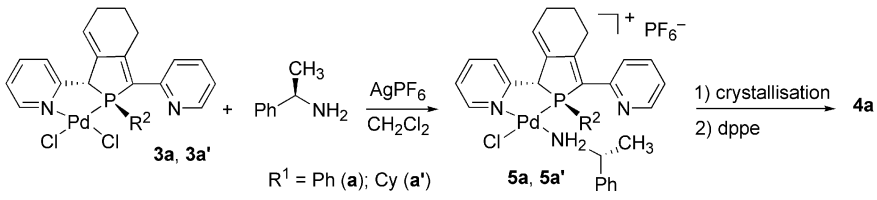

Scheme 2. Ligand-exchange reactions with 2-pyridylphospholene palladium complexes.

NMR: +89.2 and +90.2 ppm] in an 85% yield; ^{1}H and ^{13}C NMR spectroscopic data confirm the proposed structure. Quite surprisingly, this ligand-exchange reaction failed for complexes **3b**–**3c′**, which carry either dangling R^1 phenyl or 2-thienyl substituents (Scheme 1). It is worth noting that the overall transformation **1a** → **5a** could be performed in a "one-pot" approach by using (*R*)-α-methylbenzylamine both as a base to promote the phosphole–phospholene isomerisation (**2a** → **3a**, Scheme 1) and as a ligand to form **5a** as a mixture of two diastereomers (Scheme 2).

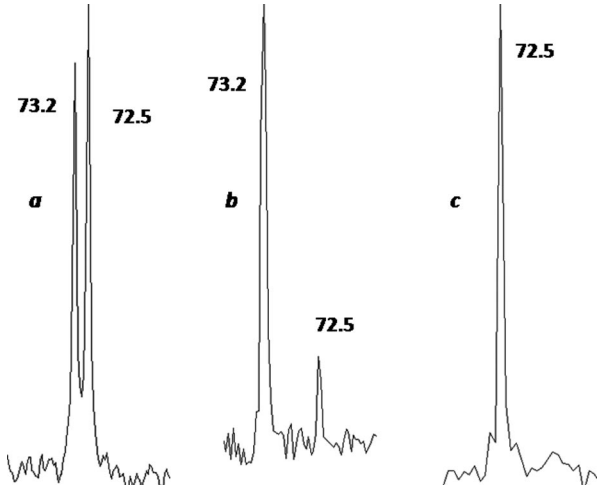

Figure 2. $^{31}P\{^{1}H\}$ NMR spectrum (+70 to +74 ppm window) of (a) the crude reaction mixture (**5a** diastereomers), (b) mother solution and (c) crystals following a single recrystallisation.

Diastereomers of **5a** were successfully separated by recrystallisation from a CH_2Cl_2 solution exposed to pentane vapour at room temperature for a week. After a single crystallisation, the mother solution was highly enriched with the diastereoisomer **5a²** (Figure 2b), while the crystals contained pure diastereoisomer **5a¹** (Figure 2c). A single-crystal X-ray diffraction study confirms the proposed structure of the optically pure complex **5a¹**. This compound crystallises in the noncentrosymmetric space group $P2_1$ of the monoclinic system. As expected, it is a monocationic complex in which the Pd^{II} metal centre is bound to the P,N chelating ligand **4a¹**, a chlorido ligand and (*R*)-α-methylbenzylamine coordinated by its terminal NH_2 group in a slightly distorted square-planar arrangement (Figure 3).

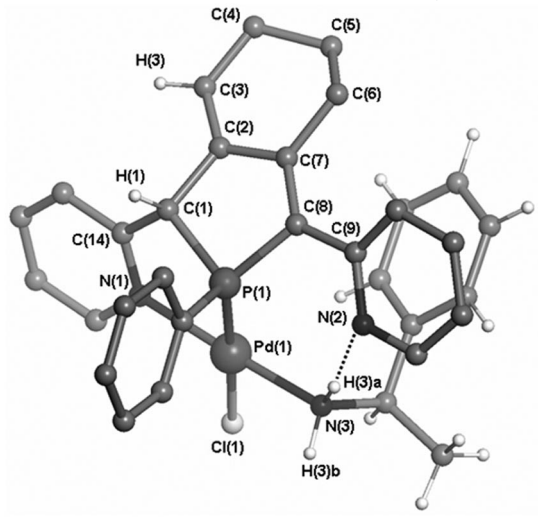

Figure 3. Molecular structure of the monocationic diastereoisomer **5a¹**. Hydrogen atoms on the phospholene ligand, with the exception of H(1) and H(3), have been omitted for clarity.

The bond lengths and angles of **5a¹** are comparable to those of related Pd^{II} 2-pyridylphospholene complexes.[7] Note that the two Pd–N bond lengths are essentially equivalent despite the different nature (sp^2/sp^3) of the N donors [2.081(3) Å (pyridine) and 2.047(3) Å (benzylamine), Table 1]. In addition, both the P- and C-stereogenic centres in ligand **4a¹** present an *S* configuration. The most remarkable structural feature of this complex, in contrast to what is expected according to the "*trans influence*", is the *trans* arrangement of the two rather "*hard*" N-donor ligands (Figure 3). The nitrogen atom of the dangling pyridyl group points towards one H atom of the amine ligand (N–H···N angle, 167.33°), and the short distance between these two centres (2.059 Å) reveals their interaction. This H-bond may be responsible both for (i) the unusual *trans* arrangement of the two N donors in the square-planar coordination sphere of the Pd^{II} centre and (ii) the fact that the ligand-exchange reaction depicted in Scheme 2 is only successful with complexes bearing a dangling pyridyl group since this H-bond helps in stabilising complexes **5a** and **5a′** (Scheme 2). The free optically pure ligand (S_C,S_P)-**4a¹** was quantitatively released by addition of 1 equiv. 1,2-(diphenyl-

Table 1. Selected bond lengths and angles for Pd^{II} complexes **3a**·1.5CH_2Cl_2,[7b] **5a¹**, Pd**1b** and Pd**4b**.

	3a·1.5CH_2Cl_2	**5a¹**	Pd**1b**	Pd**4b**
Pd(1)–P(1)	2.2123(10)	2.2237(10)	2.293(4)	2.2688(12)
Pd(1)–N(1)	2.082(3)	2.081(3)	2.138(10)	2.133(3)
Pd(1)–N(3)	–	2.047(3)	–	–
Pd(1)–Cl(1)	2.3665(11)	2.3493(11)	–	–
Pd(1)–Cl(2)	2.2950(11)	–	–	–
P(1)–Pd(1)–N(1)	84.64(9)	83.00(10)	82.7(5)	83.97(9)
P(1)–Pd(1)–N(3)	–	93.88(10)	–	–
P(1)–Pd(1)–Cl(2)	90.48(4)	–	–	–
Cl(1)–Pd(1)–N(1)	93.86(9)	93.91(10)	–	–
Cl(1)–Pd(1)–N(3)	–	89.21(10)	–	–
C(1)–P(1)–C(8)	94.20(17)	94.1(2)	91.9(7)	92.94(16)
C(100)–Pd(1)–C(102)	–	–	66.9(17)	67.47(18)

phosphanyl)ethane (dppe) to **5a**[1] (Scheme 2). Indeed, (S_C,S_P)-**4a**[1] is the first P,N-chelate-bearing an enantiopure 2-phospholene ring. This synthetic approach to P-chiral mixed phospholene–pyridine chelates failed for the corresponding P-cyclohexyl series.

Palladium Allylic Complexes

Pd-catalysed allylic substitution reactions were selected in order to evaluate the ability of the chiral pyridyl–phospholene and nonchiral pyridyl–phosphole ligands to induce regio- and enantioselectivity. Cationic (allyl)palladium complexes bearing these new P,N chelates, which are intermediates in the allylic substitution process, were thus prepared.

Complexes Pd**1b** and Pd**4b** were synthesised from the corresponding dimeric bridged palladium chloride complex in the presence of a slight excess of the appropriate P,N ligand, the pyridyl–phosphole **1b** and the racemic pyridyl–phospholene **4b** (Scheme 3), by following the methodology previously described.[12]

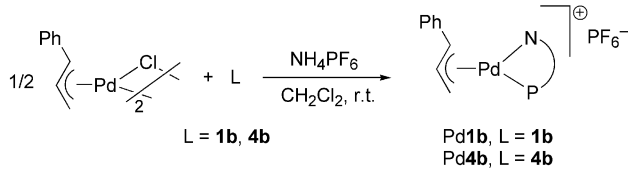

Scheme 3. Synthesis of palladium allylic complexes Pd**1b** and Pd**4b**.

The room temperature $^{31}P\{^1H\}$ NMR spectrum of complex **Pd1b** displays a singlet at +53.5 ppm, and the ^1H NMR spectrum shows broad signals for the allylic ligand. At 253 K, two signals at +53.6 ppm and +53.4 ppm appear in the $^{31}P\{^1H\}$ NMR spectrum, and the ^1H NMR signals became less broad. Two sets of signals corresponding to the allylic ligand are observed [CH_2: +3.52 and +3.90 ppm (H_{anti}); +4.80 and +4.69 (H_{syn}); PhCHC*H*: +7.09 and +6.71; PhC*H*: +5.94 and +6.14]. These data clearly show that two stereoisomers are present in solution (and each of them is a couple of enantiomers as a result of the chirality of the phosphorus atom), and the phenyl ring occupies a *syn* position with respect to the central H atom. Single crystals of **Pd1b** were successfully grown from a CH_2Cl_2 solution of the complex exposed to pentane vapours. This compound crystallises in the space group *Pna*2(1) of the orthorhombic system, and the asymmetric unit contains one monocationic complex **Pd1b** and one hexafluorophosphate counteranion (Figure 4a). The Pd^{II} centre possesses a slightly distorted square-planar geometry around it [P(1)–Pd(1)–N(1) 82.7° and C(100)–Pd(1)–C(102) 66.9(17), Table 1], and the maximum deviation from the plane defined by Pd, the N and P donors of the chelating 2-pyridylphosphole ligand and the two terminal allylic C atoms is 0.185 Å. The bond lengths and angles of the coordinated pyridyl–phosphole ligand are similar to those observed in $PdCl_2$ complexes.[7b] The bond lengths and angles of the (η^3-C_3H_5)Pd core are also consistent with known literature values.[13] A significant difference can be observed in the distances between Pd and the two terminal allylic carbon atoms [Pd–C(100) 2.0076(16) Å; Pd–C(102) 2.29(3) Å, Table 1] owing to the different *trans* effect of the N- and P-donor atoms. Finally, it is also noteworthy that (i) the phenyl substituent of the allylic ligand has a relative *cis* position with respect to the less hindered N atom and that (ii) the phenyl ring occupies a *syn* position with respect to the central allylic H atom, as observed in solution (Figure 4a).

Complex Pd**4b** bearing the phospholene ligand synthesised from **1b**, exhibits a singlet at +61.8 ppm in its room temperature $^{31}P\{^1H\}$ NMR spectrum. This chemical shift is shifted lowfield [$\Delta(\delta)$ = +8.3 ppm] relative to that of Pd**1b**, which follows the trend on going from phospholene– to phosphole–pyridine Pd^{II} complexes.[7] The structure of Pd**4b** in the solid state was established by an X-ray diffraction study (Table 1). Single crystals were obtained from diffusion of pentane vapour in a CH_2Cl_2 solution of Pd**4b**. This derivative crystallises in the *C*2/*c* space group of the monoclinic system with one monocationic palladium com-

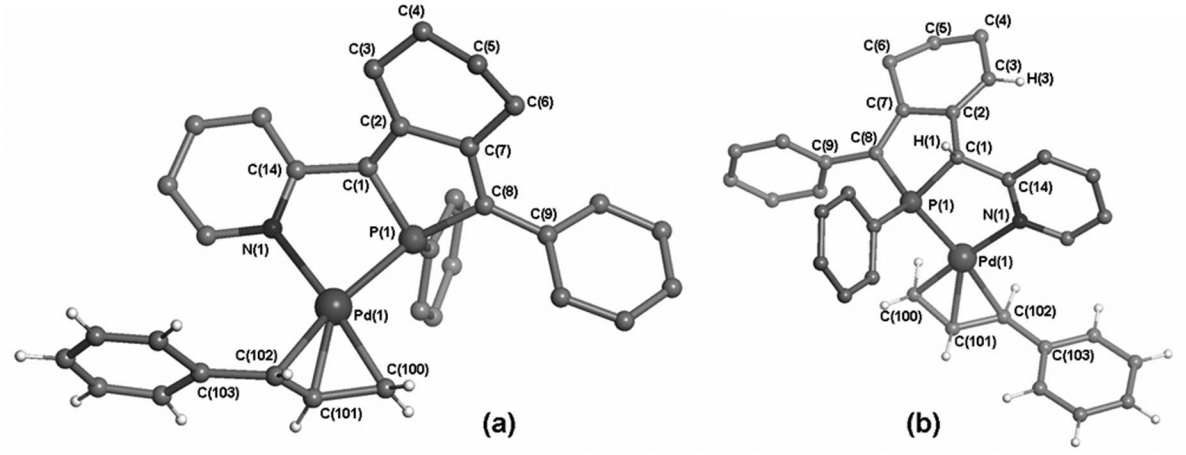

Figure 4. View of the molecular structures of complexes: (a) Pd**1b** and (b) Pd**4b**. Hydrogen atoms [with the exception of the allylic, H(1) and H(3) hydrogen atoms of **4b**] and the hexafluorophosphate anion have been omitted for clarity.

plex and one hexafluorophosphate counteranion in the asymmetric unit. This (2-pyridylphospholene) Pd^{II} complex (Figure 4b) shows a structure that is very similar to that of its phosphole-based analogue Pd**1b** (Figure 4a). Therefore, the palladium coordination sphere of Pd**4b** displays a distorted square-planar geometry, and the phenyl substituent of the allylic ligand has a *cis* configuration with respect to the N atom (Figure 4b). The Pd–N and Pd–P bond lengths, as well as the Pd–C distances involving the allylic ligand of the phospholene-containing complex Pd**4b**, are essentially comparable with those of its phosphole-based analogue Pd**1b** (Table 1).

Pd-Catalysed Allylic Substitution

Regioselective Allylic Substitution

As stated above, the allylic substitution reaction was selected to test the catalytic ability of palladium complexes bearing the newly synthesised P,N ligands. In particular, an interesting aspect of studying Pd-catalysed allylic substitutions is the regioselectivity (branched/linear ratio) for unsymmetrical substrates such as 3-acetoxy-1-phenyl-1-propene **6** and 3-acetoxy-1-methyl-1-propene **7** (Scheme 4). These alkylations were carried out using bis(trimethysilyl) acetamide (BSA) and a catalytic amount of potassium acetate as base[14] (Scheme 5). When optically pure ligands are involved, the branched isomer is desired since it contains a stereogenic C atom. This reaction was investigated by using two types of nucleophiles, namely dimethyl malonate (DMM) and benzylamine ($BnNH_2$). Furthermore, 2-pyridylphospholes and 2-pyridylphospholenes were used as ligands in order to compare the two families of related P,N chelates. The catalytic precursors were generated in situ from $[PdCl(C_3H_5)]_2$ and the appropriate ligand (Pd/L = 1:1.25).

With the phosphole-based ligands, high conversions were obtained for substrate **6** after a reaction time of 15 min (Entries 1–5, Table 2). The linear/branched ratio depends on the substitution pattern of the phosphole, and the highest selectivity in the branched derivative (*l*/*b* = 7:1) was reached with the (2-pyridyl)-capped P-cyclohexyl ligand **1a′** (Entry 2, Table 2). In contrast, with phospholene-based P,N ligands, complete conversion was only achieved with 2-(2-pyridyl)-5-phenylphospholene **4b** (Entries 6–8, Table 2). Interestingly, the selectivity towards the branched regioisomer b-**8** (*l*/*b* = 4:1) increases markedly relative to that observed with the phosphole analogues. However, this ratio

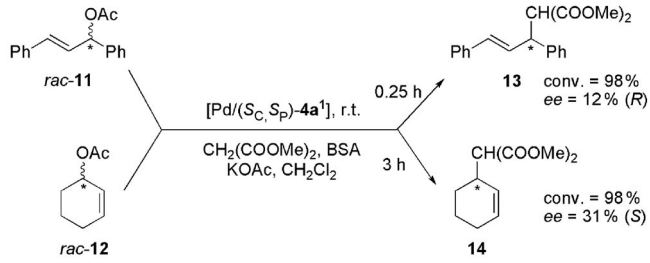

Scheme 5. Allylic alkylation of *rac*-**11** and *rac*-**12** catalysed by the Pd/(S_C,S_P)-**4a**[1] system.

remains low compared to those obtained with other P,N bidentate ligands, such as oxazolinylphosphane ligands (*l*/*b* = 1:4).[15]

Table 2. Pd-catalysed allylic substitution of **6** and **7** by using 2-pyridylphospholes and 2-pyridylphospholenes ligands.[a]

Entry	L	Substrate	NuH[b]	Time [h]	Conversion [%][c]	*l*/*b*[d]
1	**1a**	**6**	DMM	0.25	90	46:1
2	**1a′**	**6**	DMM	0.25	100	7:1
3	**1b**	**6**	DMM	0.25	91	100:0[e]
4	**1b′**	**6**	DMM	0.25	100	100:0[e]
5	**1c**	**6**	DMM	0.25	99	23:1
6	*rac*-**4a**	**6**	DMM	0.25	63	4:1
7	*rac*-**4b**	**6**	DMM	0.25	99	4:1
8	*rac*-**4b′**	**6**	DMM	0.25	34	3:1
9	**1a′**	**6**	$BnNH_2$	7	45	20:1
10	**1b**	**6**	$BnNH_2$	7	99	20:1
11	*rac*-**4b**	**6**	$BnNH_2$	7	96	9:1
12	**1b**	**7**	DMM	0.25	95	1.4:1[f]
13	*rac*-**4b**	**7**	DMM	0.25	100	2.2:1[g]

[a] Results from duplicated experiments; Pd/**L**/substrate = 1:1.25:50; see Scheme 4. [b] NuH = dimethylmalonate (DMM) with BSA and a catalytic amount of KOAc as a base; NuH = benzylamine ($BnNH_2$). [c] Conversions based on the substrate **6** or **7** determined by GC. [d] Linear/branched ratio (*l*/*b*) determined by GC. [e] Branched isomer not detected by GC. [f] l_{trans}/l_{cis} = 7:1. [g] l_{trans}/l_{cis} = 9:1.

In the allylic amination with benzylamine as a nucleophile, high conversions were reached after 7 h (Entries 9–11, Table 2). However, the major product was the linear regioisomer l-**10** (*l*/*b* ≥ 9). The highest selectivity in the branched product b-**9** was observed for the allylic alkylation of 3-acetoxy-1-methyl-1-propene **7** with both kinds of ligands – the phosphole derivative gave the best results (*l*/*b* = 1.4:1, Entry 12, Table 2). In both cases, high activity was observed with complete conversion within 15 min (Entries 12 and 13, Table 2).

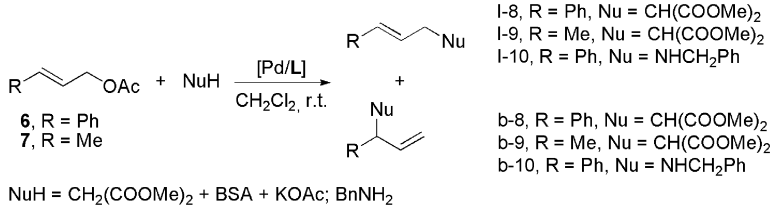

Scheme 4. Allylic substitution of **6** and **7** catalysed by Pd/**L** systems (**L** = 2-pyridylphosphole and 2-pyridylphospholene ligands).

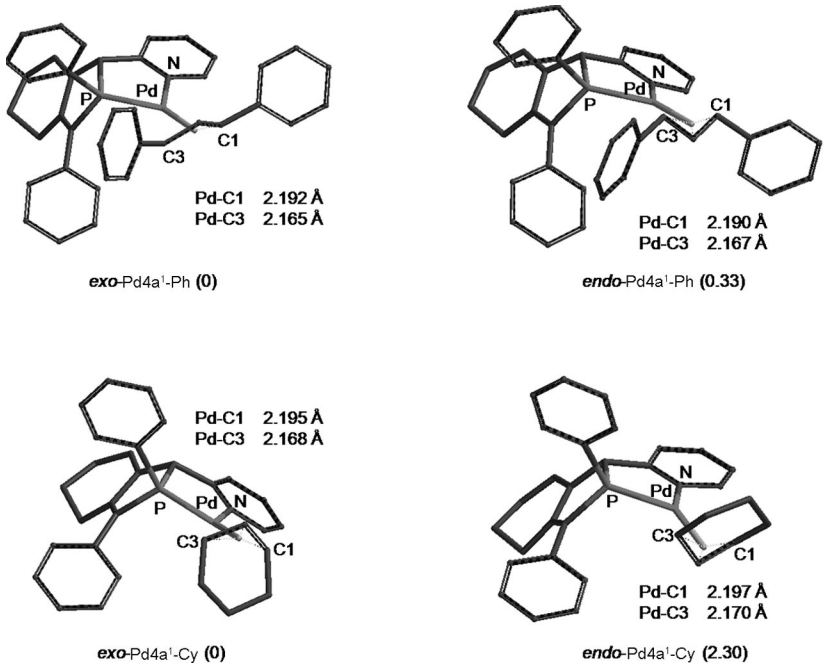

Figure 5. Modelled structures [PM3(tm)] for cationic allyl palladium complexes containing the 2-pyridylphospholene ligand **4a¹**: (top) 1,3-diphenylallyl isomers (Pd**4a¹**-Ph); (bottom) cyclohexenylallyl isomers (Pd**4a¹**-Cy). In parenthesis, relative energies calculated by DFT (in kcal/mol) are given. Hydrogen atoms are omitted for clarity.

Enantioselective Allylic Alkylation

Having one of our target enantiomerically pure 2-pyridylphospholene ligands in hand, we also investigated its use in Pd-catalysed asymmetric allylic alkylation. These alkylations were carried out with racemic 3-acetoxy-1,3-diphenyl-1-propene (*rac*-**11**) and 3-acetoxy-1-cyclohexene (*rac*-**12**) as substrates under the same basic conditions as those used for substrates **6** and **7** (Scheme 5). Catalytic precursors were generated in situ from $[PdCl(C_3H_5)]_2$ and the optically pure (S_C,S_P)-**4a¹** ligand (Pd/L = 1:1.25). For both substrates, the catalytic system was found to be very active at room temperature, which gave rise to an almost complete conversion within 15 min for *rac*-**11** and 3 h for *rac*-**12**. However, the enantiomeric excesses remain very low for this type of catalytic reaction. Note that the highest asymmetric induction (*ee* = 31%) was achieved with the less-hindered cyclic cyclohexenyl substrate.

In order to justify the different selectivities between both racemic substrates *rac*-**11** and *rac*-**12**, we calculated the equilibrium geometry and the corresponding energies for the Pd**4a¹** cationic intermediates containing 1,3-diphenylallyl (Pd**4a¹**-Ph) or cyclohexenylallyl (Pd**4a¹**-Cy) groups. In both cases, two isomers are possible because of the relative position of the central allylic carbon atom and the phenyl group bonded to the phosphorus atom: the *exo* isomer, if both groups point in the same direction as observed in the solid state (Figure 4), and the *endo* isomer, if one group points away from the other group (Figure 5). Structures of these isomers were optimised at the semiempirical PM3(tm) level, and their energies calculated by density functional methods with 6-31G* polarisation basis sets and pseudopotentials. For both types of Pd^{II} allyl complexes, the *exo* isomer is more stable than the *endo* isomer (Figure 5). The fact that the energy difference between the two cyclohexenylallyl isomers (2.3 kcal/mol) is higher than that for the corresponding 1,3-diphenylallyl isomers (0.33 kcal/mol) agrees with the higher enantiomeric excess obtained when 3-acetoxy-1-cyclohexene is used as the substrate. In addition, the absolute configuration observed for the major alkylated products, (*R*)-**13** and (*S*)-**14** is in agreement with the expected nucleophilic attack at the more electrophilic terminal allylic carbon atom placed in a position *trans* to the phosphorus atom (see calculated Pd–$C_{term\text{-}allyl}$ bond lengths in Figure 5).

Conclusions

We could obtain the optically pure 2-pyridylphospholene (S_C,S_P)-**4a¹** by resolution of a diastereomeric mixture of Pd^{II} complexes, {PdCl(κ²-*P*,*N*-**4a**)[κ¹-*N*-(*R*)-methylbenzylamine]}PF_6 (**5a**), by means of fractional crystallisation followed by reaction with 1,2-(diphenylphosphanyl)ethane, which prevents the oxidation of the ligand. Unfortunately, an analogous protocol applied to **5a′**, which features the corresponding P-cyclohexylphosphole ligand, did not work. *P*,*N*-2-Pyridylphosphole and *P*,*N*-2-pyridylphospholene ligands were tested in Pd-catalysed allylic substitutions. The nonchiral phospholes (**1a**, **1a′**, **1b**, **1b′** and **1c**) and racemic 2-phospholenes (*rac*-**4b** and *rac*-**4b′**) were used in the alkylation and amination of 3-acetoxy-1-phenyl-1-propene (**6**) and 3-acetoxy-1-methyl-1-propene (**7**), in order to evaluate their influence on regioselectivity. With *rac*-**4b** and *rac*-**4b′** phospholenes, a trend to favour the branched-substituted product was observed relative to the corresponding phos-

pholes using 3-acetoxy-1-phenyl-1-propene as substrate; however, the linear isomer was in any case the major product. With respect to the asymmetric induction, (S_C,S_P)-**4a**[1] was employed in the allylic alkylation of racemic model substrates **11** and **12**, which gives up to 31% enantiomeric excess for the less-sterically hindered substrate *rac*-3-acetoxy-1-cyclohexene (**12**). This trend could be rationalised by a modelling study of the Pd^{II} allyl intermediates responsible for the asymmetric induction.

Experimental Section

General Remarks: All compounds were prepared under a purified nitrogen atmosphere by using standard Schlenk and vacuum-line techniques. The solvents were purified by standard procedures and distilled under nitrogen.[16] [Pd(η^3-1-phenylallyl)(μ-Cl)][17] and ligands **1a**–**1c′**[7b] were prepared as described previously. NMR spectra were recorded on Varian XL-500 (^{1}H, standard $SiMe_4$), Varian Gemini (^{1}H, 200 MHz; ^{13}C, 50 MHz; standard $SiMe_4$), Bruker DRX 250 (^{13}C, 62.9 MHz, standard $SiMe_4$) and Varian Mercury 400 (^{1}H, 400 MHz; ^{13}C, 100 MHz, standard $SiMe_4$) spectrometers, with $CDCl_3$ as solvent, unless stated otherwise. Chemical shifts are reported downfield from those of the standards. IR spectra were recorded on FTIR Nicolet 520 and Nicolet 5700 spectrometers. Electron-spray mass chromatograms were obtained on a Mass ZQ Micromass instrument. High-resolution mass chromatograms were obtained on a Waters LCT Premier spectrometer operated in ESI mode. The GC analyses were performed on a Hewlett–Packard 6890-Network GC system gas chromatograph [30 m HP5 (5% phenyl)methylpolysiloxane column] with a FID detector. Enantiomeric excess was determined by HPLC on a Hewlett-Packard 1050 Series chromatograph (Chiralcel-OD chiral column) with a UV detector and by GC on a Hewlett–Packard 5890 Series II gas chromatograph [25-m FS-cyclodex-β-I/P column: heptakis(2,3,6-tri-*O*-methyl)-β-cyclodextrin/polysiloxan] with a FID detector. Elemental analyses were carried out by the Serveis Cientifico-Tècnics de la Universitat de Barcelona in an Eager 1108 microanalyzer. Modelling studies have been carried out by using the following software: SPARTAN′06 for Windows and Linux.[18]

5a: To a solution of [1-phenyl-2,5-(2-pyridyl)phosphol-2-ene]$PdCl_2$ (**3a**, 0.45 g, 0.82 mmol) in dichloromethane (5 mL), was added (+)-(*R*)-methylbenzylamine (1.5 equiv., 156 μL, 1.23 mmol). The mixture was stirred for 1 h, and dichloromethane was removed. The product was then washed with diethyl ether and dried under vacuum. Dichloromethane (5 mL) was added followed by $AgPF_6$ (1 equiv., 0.206 g, 0.82 mmol). After 4 h of stirring, the solution was filtered with Celite, and the solvent was removed to afford complex **5a** as an orange solid. Yield: 0.56 g (0.73 mmol, 89%). ^{1}H NMR (300 MHz, CD_2Cl_2): δ = 1.42 (d, $^3J_{H\text{-}H}$ = 6.5 Hz, 3 H, CH_3), 1.48 (d, $^3J_{H\text{-}H}$ = 6.9 Hz, 3 H, CH_3), 2.01–2.12 (m, 4 H, =CCH$_2$CH_2), 2.26–2.58 (m, 4 H, =CCH_2), 2.83–3.24 (m, 4 H, =CCH_2), 4.62 (d, $^2J_{P\text{-}H}$ = 13.4 Hz, 1 H, P–C*H*), 4.75 (d, $^2J_{P\text{-}H}$ = 12.6 Hz, 1 H, P–C*H*), 4.92 (m, 4 H, CH$_3$C*H* and NH_2), 5.85 (br. s, 1 H, NH_2), 6.13 (br. s, 1 H, NH_2), 6.20 (m, 1 H, C=C*H*), 6.27 (m, 1 H, C=C*H*), 7.14 (dd, $^3J_{H\text{-}H}$ = 6.3, $^3J_{H\text{-}H}$ = 6.8 Hz, 1 H, H^5 Py), 7.13–7.36 (m, 13 H, H_{arom}), 7.41–7.79 (m, 18 H, H_{arom}), 7.96 (dd, $^3J_{H\text{-}H}$ = 6.8, $^3J_{H\text{-}H}$ = 6.1 Hz, 1 H, H^4 Py), 8.13 (dd, $^3J_{H\text{-}H}$ = 6.3, $^3J_{H\text{-}H}$ = 6.5 Hz, 1 H, H^4 Py), 8.25 (m, 2 H, H^6 Py), 9.77 (d, $^3J_{H\text{-}H}$ = 7.03 Hz, 1 H, H^6 Py), 9.79 (d, $^3J_{H\text{-}H}$ = 6.8 Hz, 1 H, H^6 Py) ppm. ^{13}C{^{1}H} NMR (75.467 MHz, CD_2Cl_2): δ = 21.2 (s, C=CCH$_2$CH_2), 21.4 (s, C=CCH$_2$CH_2), 21.7 (s, CH_3), 22.9 (s, CH_3), 25.4 (s, C=CCH_2), 25.6 (s, C=CCH_2), 27.7 (d, $^3J_{P\text{-}C}$ = 10.5 Hz, C=CCH$_2$), 27.9 (d, $^3J_{P\text{-}C}$ = 10.3 Hz, C=CCH_2), 55.2 (s, CH$_3$C*H*), 55.9 (s, CH$_3$C*H*), 56.5 (d, $^1J_{P\text{-}C}$ = 38.5 Hz, P–C*H*), 56.6 (d, $^1J_{P\text{-}C}$ = 38.4 Hz, P–C*H*), 123.4 (s, C^5 Py), 123.6 (s, C^5 Py), 124.9 (d, $^3J_{P\text{-}C}$ = 7.4 Hz, C^3 Py), 125.0 (s, C^5 Py), 125.1 (d, $^3J_{P\text{-}C}$ = 7.1 Hz, C^3 Py), 125.2 (s, C^5 Py), 125.8 (d, $^3J_{P\text{-}C}$ = 13.7 Hz, C^3 Py), 125.9 (d, $^3J_{P\text{-}C}$ = 9.4 Hz, C^3 Py), 126.4 (s, *m*-C PhCHNH$_2$), 126.8 (s, *m*-C PhCHNH$_2$), 127.6 (d, $^1J_{P\text{-}C}$ = 57.8 Hz, *ipso*-C Ph), 128.6 (d, $^1J_{P\text{-}C}$ = 56.4 Hz, *ipso*-C Ph), 128.7 (s, *p*-C PhCHNH$_2$), 128.8 (s, *o*-C PhCHNH$_2$), 128.9 (s, *p*-C PhCHNH$_2$), 129.6 (d, $^3J_{P\text{-}C}$ = 11.5 Hz, *m*-C Ph), 129.6 (s, *o*-C PhCHNH$_2$), 129.8 (d, $^3J_{P\text{-}C}$ = 11.3 Hz, *m*-C Ph), 132.5 (d, $^2J_{P\text{-}C}$ = 12.9 Hz, *o*-C Ph), 132.6 (d, $^2J_{P\text{-}C}$ = 13.0 Hz, *o*-C Ph), 133.5 (d, $^4J_{P\text{-}C}$ = 3.1 Hz, *p*-C Ph), 133.6 (d, $^4J_{P\text{-}C}$ = 3.1 Hz, *p*-C Ph), 135.7 (d, $^3J_{P\text{-}C}$ = 6.5 Hz, C=*C*H), 136.0 (d, $^3J_{P\text{-}C}$ = 6.6 Hz, C=*C*H), 136.4 (d, $^2J_{P\text{-}C}$ = 11.7 Hz, PC=C_β), 136.7 (d, $^2J_{P\text{-}C}$ = 11.3 Hz, PC=C_β), 138.6 (s, C^4 Py), 138.7 (s, C^4 Py), 140.8 (s, C^4 Py), 140.9 (s, C^4 Py), 141.3 (s, *ipso*-C PhCHNH$_2$), 142.0 (s, *ipso*-C PhCHNH$_2$), 148.8 (s, C^6 Py), 149.0 (s, C^6 Py), 150.9 (d, $^2J_{P\text{-}C}$ = 9.4 Hz, C^2 Py), 151.1 (d, $^2J_{P\text{-}C}$ = 9.1 Hz, C^2 Py), 154.4 (s, C^6 Py), 154.5 (s, C^6 Py), 156.2 (d, $^2J_{P\text{-}C}$ = 12.9 Hz, PC=C_β), 157.0 (d, $^2J_{P\text{-}C}$ = 12.9 Hz, PC=C_β), 161.4 (d, $^2J_{P\text{-}C}$ = 6.8 Hz, C^2 Py), 161.6 (d, $^2J_{P\text{-}C}$ = 6.0 Hz, C^2 Py) ppm; the signal for PC_α=C is not observed. ^{31}P{^{1}H} NMR: δ = +72.5, +73.2 and –144.3 (sept, $^1J_{P\text{-}F}$ = 709 Hz) ppm. $C_{32}H_{32}ClF_6N_3P_2Pd$ (776.41): calcd. C 81.72, H 6.04, N 3.81; found C 81.65, H 6.08, N 3.75.

5a[1]: Crystallisation of complex **5a** with dichloromethane/pentane solution afforded enantiomerically pure complex **5a[1]** as orange crystals. ^{1}H NMR (200 MHz, CD_2Cl_2): δ = 1.52 (d, $^3J_{H\text{-}H}$ = 6.4 Hz, 3 H, CH_3), 1.95–2.12 (m, 2 H, =CCH$_2$CH_2), 2.26–2.54 (m, 2 H, =CCH_2), 2.83–3.16 (m, 2 H, =CCH_2), 4.65 (d, $^2J_{P\text{-}H}$ = 13.4 Hz, 1 H, P-C*H*), 4.88 (m, 2 H, CH$_3$C*H* and NH_2), 5.79 (br. s, 1 H, NH_2), 6.18 (m, 1 H, C=C*H*), 7.03–7.24 (m, 5 H, H_{arom}), 7.38–7.68 (m, 8 H, H_{arom}), 7.82–8.21 (m, 4 H, H_{arom}), 9.81 (d, $^3J_{H\text{-}H}$ = 5.5 Hz, 1 H, H^6 Py) ppm. ^{13}C{^{1}H} NMR (75.467 MHz, CD_2Cl_2): δ = 21.3 (s, C=CCH$_2$CH_2), 21.7 (s, CH_3), 25.4 (s, C=CCH_2), 27.6 (d, $^3J_{P\text{-}C}$ = 10.8 Hz, C=CCH$_2$), 55.2 (s, CH$_3$C*H*), 56.5 (d, $^1J_{P\text{-}C}$ = 38.1 Hz, P-C*H*), 123.5 (s, C^5 Py), 124.8 (d, $^3J_{P\text{-}C}$ = 7.5 Hz, C^3 Py), 125.1 (s, C^5 Py), 125.8 (d, $^3J_{P\text{-}C}$ = 13.1 Hz, C^3 Py), 126.8 (s, *m*-C PhCHNH$_2$), 127.6 (d, $^1J_{P\text{-}C}$ = 57.8 Hz, *ipso*-C Ph), 128.7 (s, *p*-C PhCHNH$_2$), 128.8 (s, *o*-C PhCHNH$_2$), 129.6 (d, $^3J_{P\text{-}C}$ = 11.2 Hz, *m*-C Ph), 132.5 (d, $^2J_{P\text{-}C}$ = 12.9 Hz, *o*-C Ph), 133.5 (d, $^4J_{P\text{-}C}$ = 3.1 Hz, *p*-C Ph), 135.7 (d, $^3J_{P\text{-}C}$ = 6.6 Hz, C=*C*H), 135.8 (d, $^1J_{P\text{-}C}$ = 6.6 Hz, PC_α=C), 136.4 (d, $^2J_{P\text{-}C}$ = 11.7 Hz, PC=C_β), 138.5 (s, C^4 Py), 140.9 (s, C^4 Py), 141.2 (s, *ipso*-C PhCHNH$_2$), 148.8 (s, C^6 Py), 150.9 (d, $^2J_{P\text{-}C}$ = 9.6 Hz, C^2 Py), 154.5 (s, C^6 Py), 156.2 (d, $^2J_{P\text{-}C}$ = 12.9 Hz, PC=C_β), 161.4 (d, $^2J_{P\text{-}C}$ = 6.4 Hz, C^2 Py) ppm. ^{31}P{^{1}H} NMR: δ = +72.5, and –143.8 (sept, $^1J_{P\text{-}F}$ = 713 Hz) ppm.

5a′: By following the procedure described for compound **5a**, reaction of complex **3a′** (0.47 g, 0.85 mmol) and (+)-(*R*)-methylbenzylamine (156 μL, 1.23 mmol) afforded compound **5a′** as an orange solid. Yield: 0.56 g (0.72 mmol, 85%). ^{1}H NMR (300 MHz, CD_2Cl_2): δ = 1.58 (d, $^3J_{H\text{-}H}$ = 6.0 Hz, 3 H, CH_3), 1.67 (d, $^3J_{H\text{-}H}$ = 6.1 Hz, 3 H, CH_3), 1.64–1.78 (m, 4 H, CH$_2$), 1.82–2.36 (m, 18 H, =CCH$_2$CH_2 and CH$_2$), 2.57–2.93 (m, 8 H, =CCH_2 and CH$_2$), 2.98–3.27 (m, 4 H, =CCH_2, CH), 4.15 (br. s, 2 H, P-C*H*), 4.75 (m, 4 H, CH$_3$C*H* and NH_2), 6.05 (m, 4 H, C=C*H*, NH$_2$), 7.14–7.53 (m, 20 H, H_{arom}), 7.92 (dd, $^3J_{H\text{-}H}$ = 5.8, $^3J_{H\text{-}H}$ = 6.8 Hz, 1 H, H^4 Py), 8.05 (dd, $^3J_{H\text{-}H}$ = 7.3, $^3J_{H\text{-}H}$ = 7.3 Hz, 1 H, H^4 Py), 8.37 (d, $^3J_{H\text{-}H}$ = 4.5 Hz, 1 H, H^6 Py), 8.53 (dd, $^3J_{H\text{-}H}$ = 4.5, $^3J_{H\text{-}H}$ = 6.5 Hz, 1 H, H^6 Py), 9.50 (d, $^3J_{H\text{-}H}$ = 5.7 Hz, 1 H, H^6 Py), 9.58 (d, $^3J_{H\text{-}H}$ = 5.9 Hz, 1 H, H^6 Py) ppm. ^{13}C{^{1}H} NMR (50.322 MHz, CD_2Cl_2): δ = 21.5 (s, C=CCH$_2$CH_2), 23.1 (s, CH_3), 23.4 (s, CH_3), 23.7 (s, CH$_2$), 24.4 (s, CH$_2$), 25.0 (s, C=CCH_2), 25.3 (s, C=CCH_2), 25.8 (d,

J_{P-C} = 7.4 Hz, CH_2), 26.2 (m, CH_2), 26.5 (d, J_{P-C} = 9.8 Hz, CH_2), 26.7 (d, J_{P-C} = 10.2 Hz, CH_2), 27.7 (s, CH_2), 27.9 (s, C=CCH_2), 28.5 (s, C=CCH_2), 35.2 (d, $^1J_{P-C}$ = 20.1 Hz, CH), 35.6 (d, $^1J_{P-C}$ = 23.5 Hz, CH), 54.8 (s, CH_3CH), 55.0 (s, CH_3CH), 54.8 (d, $^1J_{P-C}$ = 59.1 Hz, P-*C*H), 55.8 (d, $^1J_{P-C}$ = 56.2 Hz, P-*C*H), 124.0 (s, C^5 Py), 124.2 (s, C^5 Py), 124.7 (br. d, $^3J_{P-C}$ = 7.3 Hz, C^3 Py), 125.1 (s, C^5 Py), 125.2 (s, C^5 Py), 126.2 (br. d, $^3J_{P-C}$ = 12.2 Hz, C^3 Py), 126.8 (s, *m*-C $PhCHNH_2$), 127.4 (s, *m*-C $PhCHNH_2$), 129.0 (s, *p*-C $PhCHNH_2$), 129.1 (s, *p*-C $PhCHNH_2$), 129.4 (s, *o*-C $PhCHNH_2$), 129.7 (s, *o*-C $PhCHNH_2$), 135.5 (d, $^3J_{P-C}$ = 6.1 Hz, C=*C*H), 135.7 (d, $^3J_{P-C}$ = 6.3 Hz, C=*C*H), 137.1 (d, $^2J_{P-C}$ = 10.7 Hz, PC=C_β), 137.2 (d, $^2J_{P-C}$ = 10.7 Hz, PC=C_β), 138.9 (s, C^4 Py), 139.2 (s, C^4 Py), 141.3 (s, *ipso*-C $PhCHNH_2$), 142.1 (s, *ipso*-C $PhCHNH_2$), 142.6 (s, C^4 Py), 142.7 (s, C^4 Py), 149.5 (s, C^6 Py), 149.7 (s, C^6 Py), 151.7 (d, $^2J_{P-C}$ = 9.8 Hz, C^2 Py), 151.9 (d, $^2J_{P-C}$ = 10.0 Hz, C^2 Py), 154.3 (s, C^6 Py), 154.4 (s, C^6 Py), 154.9 (d, $^2J_{P-C}$ = 10.5 Hz, PC=C_β), 155.6 (d, $^2J_{P-C}$ = 10.8 Hz, PC=C_β), 162.4 (d, $^2J_{P-C}$ = 5.7 Hz, C^2 Py), 162.6 (d, $^2J_{P,C}$ = 5.6 Hz, C^2 Py), PC_α=C ppm is not observed. $^{31}P\{^1H\}$ NMR: δ = +89.2, +90.2 and –142.9 (sept, $^1J_{P-F}$ = 712 Hz) ppm.

Pd1b: Ligand **1b** (0.0844 g, 0.230 mmol) and [Pd(μ-Cl)(η^3-1-Ph-C_3H_4)]$_2$ (0.0592 g, 0.114 mmol) were dissolved in dichloromethane (20 mL) at room temperature under nitrogen overnight. NH_4PF_6 (0.122 g, 0.747 mmol) was then added, and the mixture was stirred for 24 h. After this time, the mixture was washed with degassed water (6 × 10 mL). The aqueous phase was extracted with dichloromethane (3 × 10 mL). All the organic extracts were dried with Na_2SO_4 and filtered off, and the solvent was then evaporated to afford an orange solid. The product was recrystallised from a mixture of dichloromethane and hexane (1:2). Yield: 0.100 g (65%). $C_{34}H_{31}F_6NPPd$ (735.97): calcd. C 55.49, H 4.24, N 1.90; found C 55.00, H 4.40, N 1.95. IR (KBr): $\tilde{\nu}$ = 3053, 2961, 1596, 1461, 1434, 1260, 1099, 838 (PF_6) cm^{-1}. ^1H NMR (50 MHz, [D_6]acetone, 273 K): Isomer **a** (53%), δ = 1.65–1.70 (m, 2 H), 1.97 (br. s, 2 H), 2.85 (br. s, 1 H), 2.88 (br. s, 1 H), 3.23 (br. s, 1 H), 3.25 (br. s, 1 H), 3.52 (br. s, 1 H), 4.80 (br. s, 1 H), 5.94 (br. s, 1 H), 7.09 (br. s, 1 H), 6.98–8.06 (aromatic protons, 19 H) ppm; Isomer **b** (47%): δ = 1.83 (br. s, 2 H), 1.97 (br. s, 2 H), 2.73 (br. s, 2 H), 3.42 (br. s, 2 H), 3.90 (br. s, 1 H), 4.69 (br. s, 1 H), 6.14 (br. s, 1 H), 6.71 (br. s, 1 H), 6.98–8.06 (aromatic protons, 19 H) ppm. $^{31}P\{^1H\}$ NMR (101 MHz, [D_6]acetone, 253 K): δ = –144.5 (hp, J_{P-F} = 706.0 Hz), 53.4 (s), 53.5 (s) ppm. MALDI MS: *m*/*z* = 591.7 $[M - PF_6]^+$ (calcd. for $[C_{34}H_{31}NPPd]^+$ 590.999).

Palladium-Catalysed Allylic Alkylation of *rac*-3-Acetoxy-1,3-diphenyl-1-propene (*rac*-11): The catalytic precursor was generated in situ from [Pd(η^3-C_3H_5)(μ-Cl)]$_2$ and the appropriate ligand (0.02 mmol of Pd and 0.025 mmol of the chiral ligand) in CH_2Cl_2 (2 mL) over 30 min before adding the substrate. *rac*-3-Acetoxy-1,3-diphenyl-1-propene (0.252 g, 1 mmol), dissolved in CH_2Cl_2 (2 mL), was added followed by dimethyl malonate (0.396 g, 3 mmol), BSA (0.610 mg, 3 mmol) and a catalytic amount of KOAc. The mixture was stirred at room temperature until total conversion of the substrate (monitored by TLC, unless stated otherwise). The solution was then diluted with ethyl ether, filtered through Celite and washed with saturated ammonium chloride solution (4 × 10 mL) and water (4 × 10 mL). The organic phase was dried with anhydrous Na_2SO_4 and filtered off, and the solvent was removed under reduced pressure. The product was purified by column chromatography (SiO_2; ethyl acetate). The enantiomeric excess was determined by HPLC on a Chiralcel OD column, by using hexane/2-propanol (99:1) as eluent with a flow rate of 0.3 mL/min.

Palladium-Catalysed Allylic Alkylation of *rac*-3-Acetoxy-1-cyclohexene (*rac*-12): This procedure was analogous to the one described for *rac*-3-acetoxy-1,3-diphenyl-1-propene. Purification of the product was performed by column chromatography (SiO_2; ethyl acetate). The enantiomeric excess was determined by GC on a FS-cyclodex-β-I/P column.

Table 3. Structure determination data of complexes **5a**[1], Pd**1b** and Pd**4b**.

	5a[1]	Pd**1b**	Pd**4b**
Formula	$C_{32}H_{32}ClF_6N_3P_2Pd$	$C_{34}H_{31}F_6NP_2Pd$	$C_{32}H_{31}F_6NP_2Pd$
Formula mass	776.40	735.94	735.94
T [K]	100(2)	298(2)	120(2)
Crystal size [mm]	0.15 × 0.10 × 0.05	0.12 × 0.05 × 0.05	0.20 × 0.05 × 0.05
Crystal system	monoclinic	orthorhombic	monoclinic
Space group	*P*21	*Pna*2(1)	*C*2/*c*
a [Å]	9.4880(2)	17.3602(18)	25.907(5)
b [Å]	18.1207(4)	12.9213(13)	14.068(5)
c [Å]	9.8438(2)	14.3200(15)	17.584(5)
α [°]	90	90	90
β [°]	106.4610(10)	90	98.221(5)
γ [°]	90	90	90
V [Å^3]	1623.07(6)	3212.2(6)	6343(3)
Z	2	4	4
$\rho_{calcd.}$ [Mg m^{-3}]	1.589	1.522	1.541
F(000)	784	1488	2976
μ [mm^{-1}]	0.815	0.737	0.747
θ limit [°]	3.12–27.52	2.12–28.37	2.96–27.48
Reflections collected	6859	19845	14204
Independent reflections	6859	5966	7252
Reflections [$I > 2\sigma(I)$]	6257	5966	5339
Data/restraints/parameters	6859/1/407	5966/1/398	7252/0/414
GoF on F^2	1.109	0.977	1.028
Final *R* indices [$I > 2\sigma(I)$]	*R*1 = 0.0403, *wR*2 = 0.1022	*R*1 = 0.0689, *wR*2 = 0.1552	*R*1 = 0.0514, *wR*2 = 0.1407
R indices (all data)	*R*1 = 0.0466, *wR*2 = 0.1072	*R*1 = 0.2272, *wR*2 = 0.2351	*R*1 = 0.0717, *wR*2 = 0.1594
Absolute structure parameter	0.00	–0.04(8)	–
Largest diff. peak and hole [e Å^{-3}]	1.065 and –0.479	1.102 and –0.603	0.907 and –1.009

Palladium-Catalysed Allylic Alkylation of (*E*)-3-Acetoxy-1-phenyl-1-propene (6) and (*E*)-3-Acetoxy-1-methyl-1-propene (7): This procedure was analogous to the one described for *rac*-3-acetoxy-1,3-diphenyl-1-propene. The product was purified by column chromatography (SiO_2; ethyl acetate). Regioselectivity was determined by GC.

X-ray Crystallographic Study: Crystals of **5a[1]**, Pd**1b** and Pd**4b** were selected and mounted on a Bruker SMART-CCD-1000 area detector single-crystal diffractometer (Pd**1b**) with graphite monochromatised Mo-K_α radiation (λ = 0.71073 Å) or on an APEX II Bruker-AXS (Centre de Diffractométrie, Université de Rennes 1, France) (**5a[1]**, Pd**4b**) with graphite monochromatised Mo-K_α radiation (λ = 0.71073 Å). Crystal data are summarised in Table 3. Preliminary unit-cell constants were calculated with a set of 45 narrow frame (0.3° in ω) scans. The reflections were indexed, corrected for Lorentz-polarisation and integrated with the DENZO program of the KappaCCD software package.[19] The data merging process was performed by using the SCALEPACK program.[20] Structure determinations were performed by direct methods with the solving programs SHELXS[21] or SIR97,[22] which revealed all the non-hydrogen atoms. The SHELXL program was used to refine the structures by full-matrix least-squares based on F^2.[21] All non-hydrogen atoms were refined with anisotropic displacement parameters. Hydrogen atoms were included in idealised positions and refined with isotropic displacement parameters. CCDC-746795 (for **5a[1]**), 746796 (for Pd**1b**) and -746797 (for Pd**4b**) contain the supplementary crystallographic data for this paper. These data can be obtained free of charge from The Cambridge Crystallographic Data Centre via www.ccdc.cam.ac.uk/data_request/cif.

Acknowledgments

The authors wish to thank Prof. Agusti Lledós for fruitful discussions on modelling palladium complexes and the Ministerio de Educación y Ciencia (CTQ2007–61058/BQU), the Generalitat de Catalunya and CNRS for financial support.

[1] I. Ojima (Ed.), *Catalytic Asymmetric Synthesis*, 2nd ed., Wiley-VCH, New York, **2000**.
[2] For nontraditional approaches to asymmetric catalysis, see: P. J. Walsh, M. C. Kozlowski in *Fundamentals of Asymmetric Catalysis* (Foreword: D. A. Evans), University Science Book, Sausalito, **2009**, pp. 191–230.
[3] E. M. Jacobsen, A. Pfaltz, H. Yamamoto (Eds.), *Comprehensive Asymmetric Catalysis*, Springer-Verlag, Berlin, **1999**.
[4] M. J. Burk, J. E. Feaster, R. L. Harlow, *Organometallics* **1990**, *9*, 2653–2655.
[5] Selected review contributions: a) T. P. Clark, C. R. Landis, *Tetrahedron: Asymmetry* **2004**, *15*, 2123–2137; b) M. J. Burk, J. A. Ramsden in *Handbook of Chiral Chemicals* (Ed.: D. Ager), 2nd ed., CRC Press LLC, Boca Raton, **2006**, pp. 249–268; c) M. J. Burk, *Acc. Chem. Res.* **2000**, *33*, 363–372.
[6] Selected reviews: a) C. Lescop, M. Hissler in *Tomorrow's Chemistry Today* (Ed.: B. Pignataro), Wiley-VCH, New York, **2008**, pp. 295–319; b) F. Mathey (Ed.), *Phosphorus-Carbon Heterocyclic Chemistry: The Rise of a New Domain*, Pergamon, Oxford, **2001**; c) K. M. Pietrusiewicz, M. Zablocka, *Chem. Rev.* **1994**, *94*, 1375–1411.
[7] a) F. Leca, M. Sauthier, B. le Guennic, C. Lescop, L. Toupet, J.-F. Halet, R. Réau, *Chem. Commun.* **2003**, 1774–1775; b) F. Leca, C. Lescop, L. Toupet, R. Réau, *Organometallics* **2004**, *23*, 6191–6201; c) Z. Pakulski, O. M. Demchuk, J. Frelek, R. Luboradzki, K. M. Pietrusiewicz, *Eur. J. Org. Chem.* **2004**, 3913–3918; d) Z. Pakulski, R. Kwiatosz, K. M. Pietrusiewicz, *Tetrahedron* **2005**, *61*, 1481–1492.
[8] For a key contribution, see: B. M. Trost, C. Lee in *Catalytic Asymmetric Synthesis* (Ed.: I. Ojima), 2nd ed., Wiley-VCH, New York, **2000**.
[9] a) J. Hydrio, M. Gouygou, F. Dallemer, J.-C. Daran, G. G. A. Balavoine, *Tetrahedron: Asymmetry* **2002**, *13*, 1097–1102; b) J. G. Lopez Cortes, O. Ramon, S. Vincendeau, D. Serra, F. Lamy, J.-C. Daran, E. Gouygou, *Eur. J. Inorg. Chem.* **2006**, 5148–5157.
[10] J. Wassenaar, S. van Zutphen, G. Mora, P. Le Floch, M. A. Siegler, A. L. Spek, J. N. H. Reek, *Organometallics* **2009**, *28*, 2724–2734.
[11] Selected contributions: a) P. Dierkes, S. Ramdeehul, L. Barloy, A. De Cian, J. Fischer, P. C. J. Kamer, P. W. N. M. van Leeuwen, J. A. Osborn, *Angew. Chem. Int. Ed.* **1998**, *37*, 3116–3118; b) J.-L. Vasse, R. Stranne, R. Zalubovskis, C. Gayet, C. Moberg, *J. Org. Chem.* **2003**, *68*, 3258–3270; c) Z. Chen, Q. Jiang, G. Zhu, D. Xiao, P. Cao, C. Guo, X. Zhang, *J. Org. Chem.* **1997**, *62*, 4521–4523; d) T. P. Clark, C. R. Landis, *J. Am. Chem. Soc.* **2003**, *125*, 11792–11793.
[12] a) P. von Matt, G. C. Lloyd-Jones, A. B. E. Minidis, A. Pflatz, L. Macko, M. Neuburger, M. Zehnder, H. Rüegger, P. S. Pregosin, *Helv. Chim. Acta* **1995**, *78*, 265–284; b) M. Gómez, S. Jansat, G. Muller, M. A. Maestro, J. Mahía, M. Font-Bardia, X. Solans, *J. Chem. Soc., Dalton Trans.* **2001**, 1432–1439.
[13] a) M. Kollmar, B. Goldfuss, M. Reggelin, F. Rominger, G. Helmchen, *Chem. Eur. J.* **2001**, *7*, 4913–4927; b) M. Kollmar, H. Steinhagen, J. P. Janssen, B. Goldfuss, S. A. Malinovskaya, J. Vázquez, F. Rominger, G. Helmchen, *Chem. Eur. J.* **2002**, *8*, 3103–3114; c) D. Franco, M. Gómez, F. Jiménez, G. Muller, M. Rocamora, M. A. Maestro, J. Mahía, *Organometallics* **2004**, *23*, 3197–3209.
[14] B. M. Trost, D. J. Murphy, *Organometallics* **1985**, *4*, 1143–1145.
[15] a) G. Helmchen, A. Pfaltz, *Acc. Chem. Res.* **2000**, *33*, 336–345; b) P. G. Cozzi, N. Zimmermann, R. Hilgraf, S. Schaffner, A. Pfaltz, *Adv. Synth. Catal.* **2001**, *343*, 450–454.
[16] W. L. F. Armarego, D. D. Perrin in *Purification of Laboratory Chemicals*, 4th ed., Butterworth-Heinemann, Oxford, U. K., **1996**.
[17] Y. Tatsuno, T. Yoshida, S. Otsuka, *Inorg. Synth.* **1990**, *28*, 342–344.
[18] *SPARTAN'06 for Windows and Linux*, Wavefunction, Inc. 18401 Von Karman Avenue, suite 370, Irvine, CA 92612, USA, **2006**.
[19] *Area-Detector Integration Software*, Siemens Industrial Automation, Inc., Madison, WI, **1995**.
[20] Z. Otwinowski, W. Minor in *Methods in Enzymology* (Ed.: C. W. Carter Jr, R. M. Sweet), New York, Academic Press, **1997**, *276*, p. 307.
[21] G. M. Sheldrick, *SHELX97, Program for the Refinement of Crystal Structures*, University of Göttingen, Germany, **1997**.
[22] A. Altomare, M. C. Burla, M. Camalli, G. Cascarano, C. Giacovazzo, A. Guagliardi, A. G. G. Moliterni, G. Polidori, R. Spagna, *J. Appl. Crystallogr.* **1999**, *32*, 115–119.

Received: September 8, 2009
Published Online: November 11, 2009

